第 30 卷第 8 期
2014 年 8 月

无 机 化 学 学 报
CHINESE JOURNAL OF INORGANIC CHEMISTRY

Vol.30 No.8
1961-1968

$CoFe_2O_4$ 纳米晶与牛血清白蛋白和牛血红蛋白的相互作用：吸附、纳米晶的团聚及蛋白构象的变化

李 强[1] 姬晓旭[2] 张 凯[3] 黄新堂*,[1] 熊 丽*,[3]

([1]华中师范大学纳米科技研究院,武汉 430079)

([2]南阳师范学院物理与电子工程学院,南阳 473061)

([3]湖北省遗传调控与整合生物学重点实验室,华中师范大学生命科学学院,武汉 430079)

摘要：水热制备了约 10 nm 的 $CoFe_2O_4$ 纳米晶,通过 Zeta 电势、动态光散射(Dynamic Light Scattering,DLS)和傅立叶变换红外光谱(FTIR)技术研究了纳米晶与牛血清白蛋白(Bovine Serum Albumin,BSA)和牛血红蛋白(Hemoglobin)的相互作用。纳米晶对 BSA 和血红蛋白都有很强的吸附,其中对血红蛋白的吸附符合静电吸附的规律,而对 BSA 的吸附则不符合静电吸附的规律。在 pH=5.5 和 7.0 时纳米晶对 BSA 和血红蛋白的吸附容量分别达到 237.9 $mg\cdot g^{-1}$ 和 256.9 $mg\cdot g^{-1}$。DLS 结果表明蛋白质能够导致纳米晶团聚。吸附 BSA 或血红蛋白后,纳米晶的 DLS 粒径由 51 nm 分别增大到 472 nm 和 114 nm。$CoFe_2O_4$ 纳米晶还导致了蛋白质 FTIR 谱发生明显变化。BSA 和血红蛋白的酰胺 I 带由于纳米晶的作用分别减少了 4 cm^{-1} 和 6 cm^{-1}。

关键词：$CoFe_2O_4$ 纳米晶；BSA；牛血红蛋白；相互作用

中图分类号：O614.81+2；TM277+.1；Q51 **文献标识码**：A **文章编号**：1001-4861(2014)08-1961-08

DOI:10.11862/CJIC.2014.219

Interactions of $CoFe_2O_4$ Nanocrystals with Bovine Serum Albumin and Hemoglobin: Adsorption, Aggregation and Protein Conformational Changes

LI Qiang[1] JI Xiao-Xu[2] ZHANG Kai[3] HUANG Xin-Tang*,[1] XIONG Li*,[3]

([1]*Institute of Nanoscience and Nanotechnology, Central China Normal University, Wuhan* 430079, *China*)

([2]*School of Physics and Electronic Engineering, Nanyang Normal University, Nanyang, Henan* 473061, *China*)

([3]*Hubei Key Laboratory of Genetic Regulation and Integrative Biology, College of Life Sciences, Central China Normal University, Wuhan* 430079, *China*)

Abstract: Cobalt ferrite ($CoFe_2O_4$) nanocrystals (approximately 10 nm) were prepared by hydrothermal method and their interactions with Bovine Serum Albumin (BSA) and bovine hemoglobin were investigated by Zeta potential, Dynamic Light Scattering (DLS) and FTIR Spectroscopy techniques. Results show that nanocrystal-hemoglobin adsorption correlates to electrostatic attractive/repulsive interaction, whereas BSA does not follow this scheme. The corresponding adsorption capacity of BSA and hemoglobin reaches a maximum value of 237.9 $mg\cdot g^{-1}$ and 256.9 $mg\cdot g^{-1}$ at pH value of 5.5 and 7.0, respectively. DLS measurements indicate that protein adsorption have led to nanocrystal-protein aggregates formation. Comparing to the hydrodynamic size of bare nanocrystals (51 nm), that for BSA and hemoglobin increases to 472 nm and 114 nm respectively upon protein adsorption. The interaction with nanocrystal also induces protein conformation changes. The amide I band in IR spectrum shifts 4 cm^{-1} and 6 cm^{-1}, respectively, to lower wavenumbers in the case of BSA and hemoglobin.

Key words: $CoFe_2O_4$ nanocrystal; BSA; hemoglobin; interaction

收稿日期:2013-12-28。收修改稿日期:2014-03-26。

国家自然科学基金(No.51172085)资助项目。

*通讯联系人。E-mail:xthuang@phy.ccnu.edu.cn

0 Introduction

With the development of nanotechnology and its applications in biological fields, the search for understanding protein-nanoparticle interactions has drawn much attention because it has significant impact on the biological responses to nanoparticles[1-6]. When nanomaterials are exposed to physiological medium, interactions with proteins will lead to the formation of a protein corona on the nano-surface, which is responsible for the biological behaviors such as cellular uptake, endocytosis, pinocytosis, cellular recognization, cellular organelles distribution and in vivo biocompatibility/toxicity[1-8] etc. In addition, this interaction is also a key factor determining the biological applications of nanomaterials including biosensor[9-12], protein carrier[13], nanomaterial preparation[14], bio-conjugation[15-16] and nanoproteomics[17]. Therefore, understanding protein-nanoparticle interaction phenomena and associated mechanism will be essential to the development of nanotechnology in biological fields. Many previous studies have revealed that protein-nanoparticle interaction is controlled by the forces existing at nano-bio interface, such as electrostatic interaction, hydrophilic/hydrophobic interactions, van der Waals and solvation [2-3] etc. Among them, electrostatic interaction is a major force governing interactions between hydrophilic nanomaterials and protein molecules[18-19]. If protein-nanoparticle is governed by electrostatic interaction, protein adsorption will be only observed between oppositely charged nanoparticles and protein molecules because of the attractive force of opposite charges, otherwise non-electrostatic interaction will play a more important role[18-19]. In the context of experimental approaches, ζ potential correlates to the electrostatic states of nanoparticle and protein molecule and its value can be easily varied by the pH condition and then measured by instrument[18-20]. Therefore, electrostatic interaction governed protein-nanoparticle adsorption can be inferred from the correlations between protein adsorption and ζ potentials of protein-nanoparticle system at different pH conditions[18]. In addition to the above mentioned techniques, Dynamic Light Scattering (DLS) is another approach for protein-nanoparticle interaction research. When proteins are adsorbed to a nanoparticle, the hydrodynamic diameter changes arising from protein-nanoparticle interaction can be easily measured by DLS technique[2]. Interactions with nanoparticle also induce protein conformation changes, which can be detected by FTIR Spectroscopy[2].

As an important ferrite nanomaterial, cobalt ferrite ($CoFe_2O_4$) nanostructures have potential applications in biological fields such as antibacteria[21-22], hyperthermia[23-24], magnetic resonance imaging (MRI)[25-26], drug delivery[27] and anticancer[28] etc. However, very little is known about the interaction details between $CoFe_2O_4$ nanoparticles and proteins. In this work, the interactions of hydrothermally prepared $CoFe_2O_4$ nanocrystals with protein are investigated using BSA and hemoglobin as model proteins.

1 Experimental

1.1 Preparation and characterization of ultrafine $CoFe_2O_4$ nanocrystals

Ultrafine $CoFe_2O_4$ nanocrystals were synthesized by hydrothermal method. In a typical synthesis, 10 mmol $FeCl_3 \cdot 6H_2O$ and 5 mmol $CoCl_2 \cdot 6H_2O$ were dissolved in 50 mL deionized water, and then adjusted the pH value to 8.0 using ammonia solution. After magnetic stirring for several minutes, the colloidal solution was sealed in an 80 mL Teflon-lined autoclave and maintained at 190 ℃ for 10 h. The product was collected and thoroughly washed with deionized water, then dried at 60 ℃.

The morphologies of $CoFe_2O_4$ nanocrystals were observed by high-resolution transmission electron microscopy (HRTEM, JEOL JEM-2010FEF, 200 kV). Crystalline phase was identified by X-ray diffraction (XRD) method on a PANalytical X′ Pert Pro diffractometer equipped with PIXcel^{3D} detector and Cu $K\alpha$ radiation (λ=0.154 18 nm, Ni filter). Applied voltage and current was 40 kV and 40 mA respectively. The incident light divergent slit size, diffracted beam anti-scatter slit size and receiving slit size was 0.5°, 2° and 0.1 mm respectively. The scan step size was

0.026°·s^{-1}. The patterns were recorded in the 2θ range of 10°~80°. The elements composition was determined by Energy Dispersive X-ray spectroscopy (AMETEK).

1.2 Protein adsorption to $CoFe_2O_4$ nanocrystals and the correlations to Zeta potentials

$CoFe_2O_4$ nanocrystals amounts corresponding to a concentration of 1, 2, 3, 4 and 5 mg·mL^{-1} were respectively dissolved in 5 mL sodium acetate buffered (sodium acetate, 10 mmol·L^{-1}) protein solution (containing 0.5 mg·mL^{-1} BSA or hemoglobin). After shaking for five minutes, the nanocrystals were removed by centrifugation (10 000 r·min^{-1} for 3 min). Unbounded protein in supernatant was determined by Bradford method[29]. Experiments were respectively carried out under a pH value of 4.8, 5.5, 7.0 and 8.0 for understanding the pH effects. Adsorption percentages at different nanocrystal concentrations were calculated by equation $(C_0-C_e)/C_0\times100\%$, where C_0 is the initial protein concentration (0.5 mg·mL^{-1}), C_e is the unbounded protein concentration in supernatant. Adsorption capacities (mg of protein per gram of nanoparticles) corresponding to different C_{nano} were calculated by equation $1\ 000[(C_0-C_e)/C_{nano}]$ ($C_e\neq0$), where C_{nano} is the nanocrystal concentration. After that, all the adsorption capacities corresponding to one pH point was averaged. In order to elucidating adsorption mechanism, ζ potentials of nanocrystals, BSA and hemoglobin were measured by Marlven ZEN3690 at the pH value of 4.8, 5.5, 7.0 and 8.0.

1.3 DLS analysis of nanocrystals-protein interaction

Hydrodynamic diameters of bare or protein loaded nanocrystals were detected by Marlven ZEN3690. In order to directly observe the morphologies of protein loaded nanocrystals, SEM images of nanocrystals were obtained after protein adsorption by SEM JOEL JSM-6700F (10.0 kV).

1.4 FTIR spectroscopy of nanocrystals-protein interaction

After thoroughly washed with deionized water, protein loaded nanocrystals were freeze-dried at −60 ℃ to remove water. About 1% sample was homogeneously mixed with KBr, then pressed to a pellet. The FTIR spectrum was recorded at a FTIR spectrometer Avatar 360. For comparing FTIR changes induced by nanocrystals, the FTIR spectra of bare nanocrystals, BSA and hemoglobin were also recorded by the same method.

2 Results and discussion

2.1 Characterizations of $CoFe_2O_4$ nanocrystals

HRTEM, XRD and EDX characterizations are shown in Fig.1. All the peaks in XRD pattern are indexed well to the spinel phase of $CoFe_2O_4$ (PDF No. 79-1744). Nanocrystal morphology is uniform sphere with an approximate size of 10 nm. The lattice interplanar spacing (0.30 nm) in HRTEM is corresponding to the diffraction peak of lattice plane (220) in the XRD pattern (Fig.1b). EDX spectrum indicates that the atomic ratio of Co/Fe is well consistent with the molar ratio of Co/Fe in formula $CoFe_2O_4$ (Fig.1d). Above results indicate that as-prepared products are spinel phase $CoFe_2O_4$ nanocrystals with nanoscale of ~10 nm.

2.2 Protein adsorption and correlations to Zeta potentials

Protein adsorption amount as a function of pH value is shown in Fig.2. It can be found that pH value has very little impact on BSA adsorbing to nanocrystals. Although the pH value is varied from 4.8 to 8.0, BSA still can be quickly and completely removed as nanocrystal concentration is increased from 1 mg·mL^{-1} to 5 mg·mL^{-1} (Fig.2a). The calculated adsorption capacity in Fig.2b also indicates that the effect of pH value on BSA adsorption is very limited because the capacity is not remarkably varied with the pH value. On the contrary, pH condition has significant impact on nanocrystal-hemoglobin adsorption process. Adsorption percentages at pH value of 4.8 and 5.5 are close to zero indicating that hemoglobin is not removed at these conditions. Very low adsorption capacities (8.9 mg·g^{-1} and 10.0 mg·g^{-1}) also indicate that hemoglobin is not adsorbed by nanocrystals. However, hemoglobin can be efficiently adsorbed when pH value is changed to 7.0 or 8.0. Adsorption percentage quickly increases from about 60% to 100%

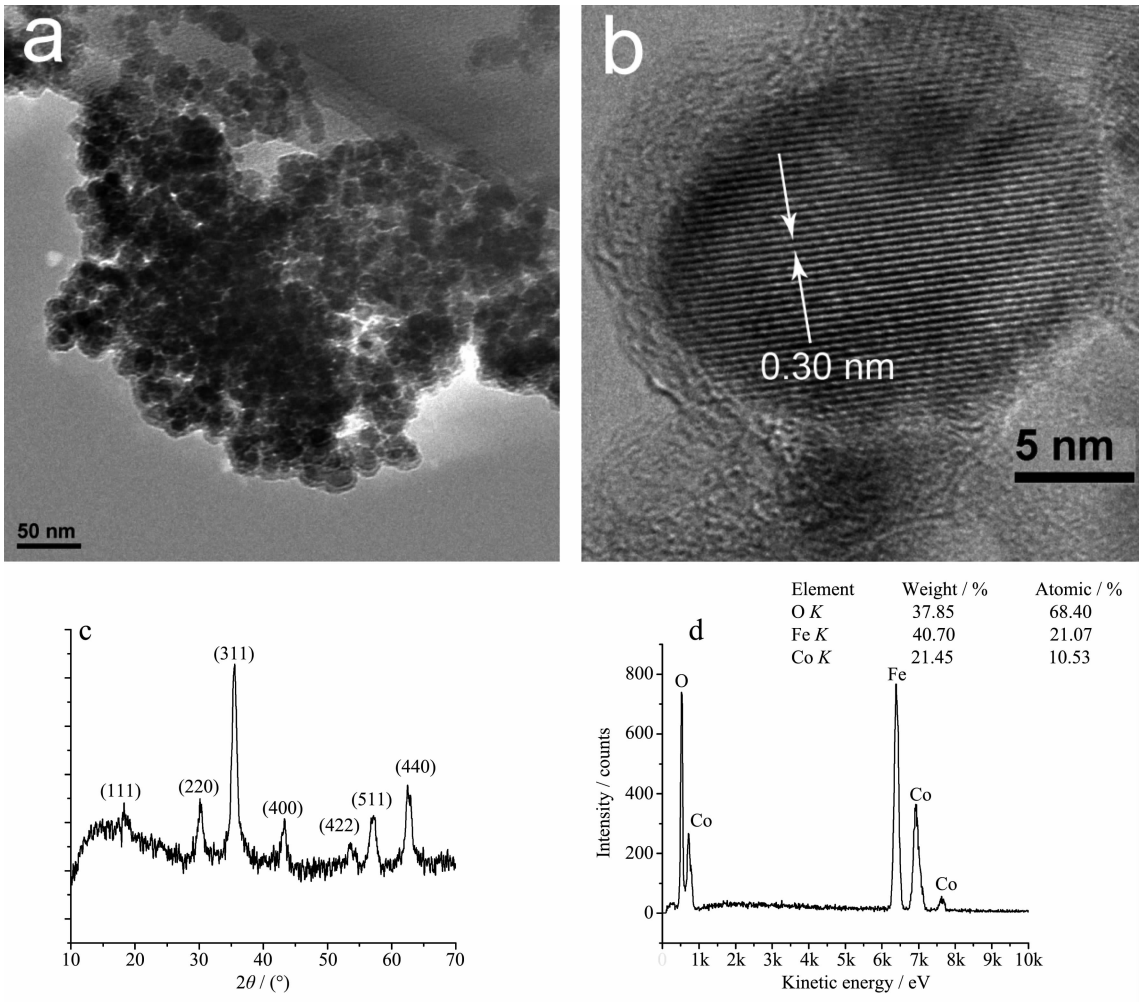

Fig.1 Characterizations of $CoFe_2O_4$ nanocrystals: (a) TEM image; (b) HRTEM image; (c) XRD pattern; (d) EDX spectrum

with nanocrystal concentration increasing from 1 mg·mL^{-1} to 3 mg·mL^{-1}. The corresponding adsorption capacity at these conditions is 256.9 mg·g^{-1} and 249.3 mg·g^{-1} respectively, which is much higher than that for pH value of 4.8 and 5.5.

In order to understand protein adsorption mechanism, ζ potentials of BSA, hemoglobin and nanocrystals are measured and presented in Fig.3. $CoFe_2O_4$ nanocrystals have a positive ζ potential approximate 20 mV with a little fluctuation at pH value of 4.8, 5.5, 7.0 and 8.0, respectively, which reveals that pH condition has no significant impact on the electrostatic state of nanocrystals. On the contrary, pH condition has remarkable effect on the electrostatic state of BSA and hemoglobin. BSA is positively charged at pH value of 4.8 but negatively charged at the pH value exceeding 5.5. Hemoglobin is positively charged with nearly the same ζ potentials (19.1 mV and 19.0 mV) at pH value of 4.8 and 5.5, but negatively charged when pH value is changed to 7.0 or 8.0.

Comparing protein adsorption and Zeta potential in Fig.2 and 3, a correlation of the electrostatic states and the adsorbed protein amount can be found. Negatively charged hemoglobin adsorbs to positively charged nanocrystals at pH value of 7.0 and 8.0, whereas no adsorption is observed for likely charged hemoglobin and nanocrystals at pH value of 4.8 and 5.5. It can be concluded that such adsorption process is highly correlated to electrostatic attractive/repulsive interaction. In contrast to hemoglobin, BSA does not follow this scheme. ζ potential differences between nanocrystals and BSA are significantly varied with pH values at the range of 4.8~8.0. But the adsorption

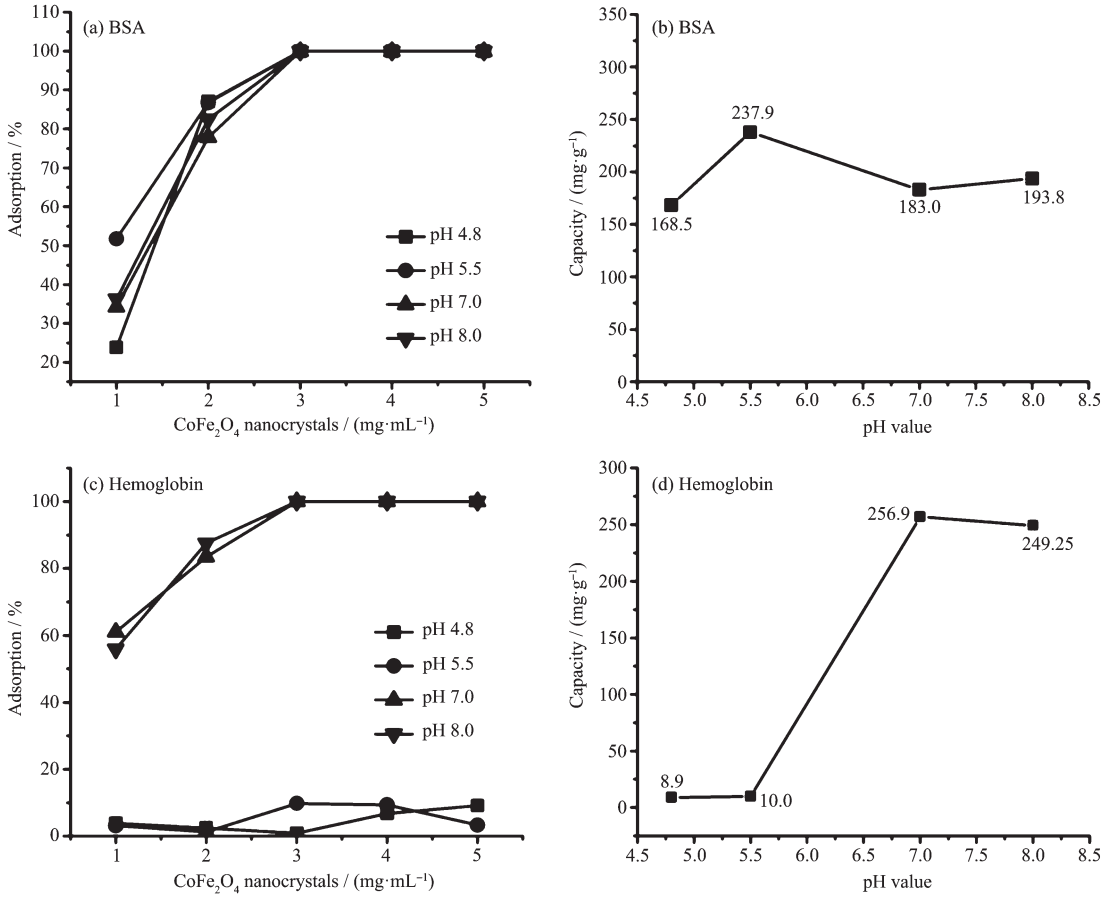

Fig.2　Protein adsorption behaviors at different pH conditions: (a) BSA adsorption percentage; (b) BSA adsorption capacity; (c) Hemoglobin adsorption percentage; (d) Hemoglobin adsorption capacity

capacities are not correlated to such changes. Even though the BSA has the same sign of surface charge to nanocrystals at pH value of 4.8, it can be adsorbed to nanocrystals with high amount of 168.5 mg·g^{-1}. When the pH values are changed to 7.0 and 8.0, BSA possesses high amount negative charges and the ζ potential differences between BSA and nanocrystals are as high as 37.2 mV and 33 mV respectively. In the context of electrostatic interaction, protein adsorption capacities should be much higher at these pH conditions. However, the experiment results are close to the adsorption capacity of pH 4.8. Therefore, BSA adsorption process could not be only explained by electrostatic interaction. This non-electrostatic interaction may be attributed to hydrophobic interaction or uneven surface charge distribution of protein molecules reported in literatures[18-19].

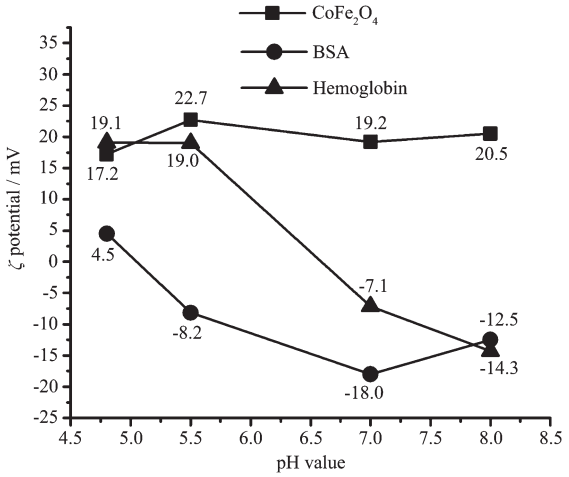

Fig.3　Zeta potentials of $CoFe_2O_4$ nanocrystals, BSA and hemoglobin at pH value of 4.8, 5.5, 7.0 and 8.0

2.3　DLS analysis of nanocrystal-protein aggregation

Nanoparticles are undergoing Brownian motion after being dispersed in solution. The hydrodynamic diameter d_H correlates to Brownian motion via Stokes-Einstein relationship. If the Brownian motion can be

measured, the d_H will be obtained. DLS is just the technique providing access to d_H through Brownian motion detection using laser technique[2]. When protein molecules bound to nanoparticles, the Brownian motion will be slowed down and consequently leading to a bigger DLS size than that of bare nanoparticles. DLS also has the ability to distinguish dimers, oligomers or aggregates of nanoparticles because of their different hydrodynamic diameters[30]. The DLS size of bare or protein loaded nanocrystals are presented in Fig.4. Bare nanocrystal has a DLS size of 51 nm, which is bigger than its real size (TEM size). This difference may be attributed to the hydration/solvation shells on the surface of nanocrystals as reported in literature[31]. After BSA adsorption, the size distribution is divided into three peaks corresponding to the mean size of 83 nm, 472 nm and 2 624 nm respectively. The size 472 nm and 2 624 nm indicate that BSA adsorption has led to aggregates of nanocrystal-BSA complex because of the much larger size than bare nanocrystal. The particle size of 83 nm may be attributed to single nanocrystal-BSA complex because it is bigger than 51 nm (bare nanocrystal) and smaller than the double nanocrystal -BSA complex of 51 nm. The intensity of particle size 472 nm is much stronger than others indicating that most of nanocrystal-BSA complex exist as moderate aggregates while very little complex exists as monomers or agglomeration. Hemoglobin adsorption leads to two particle size of 114 nm and 2 780 nm. The intensity of size 114 nm is much stronger than that of size 2 780 nm indicating that nanocrystal-hemoglobin complex mainly forms small aggregates but very little agglomeration. Comparing nanocrystal size before and after protein adsorption, there are differences in size distribution in the case of BSA and hemoglobin, which may be originated from different mechanisms of nanocrystal–protein interactions.

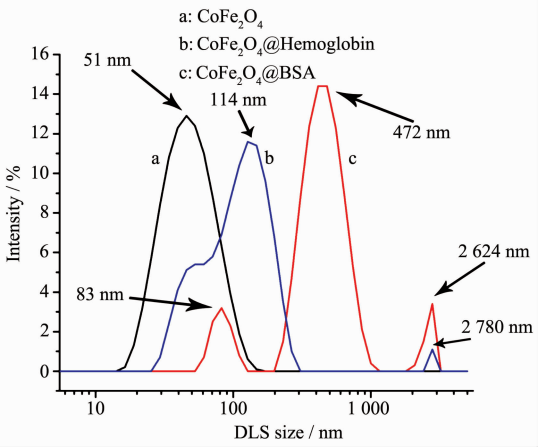

Fig.4 DLS size distribution of bare and protein attached $CoFe_2O_4$ nanocrystals

The SEM morphologies of bare and protein adsorbed nanocrystals are presented in Fig.5. Bare nanocrystal is uniform sphere with nanoscale about 10 nm (Fig.5a). The particle boundary can be clearly seen before protein binding. After protein adsorption to nanocrystals, the particle size increases and the boundary blurs due to high amount of protein coverage on the surface of nanocrystals and then aggregation of particles (Fig.5b and 5c). In summary, SEM morphologies further confirm the existence of nanocrystal-protein complex aggregates. Protein induced particle aggregation has been reported in some literatures, in which the mechanism is that protein molecules bridge particles each other to form larger nanoparticle-protein aggregates[32].

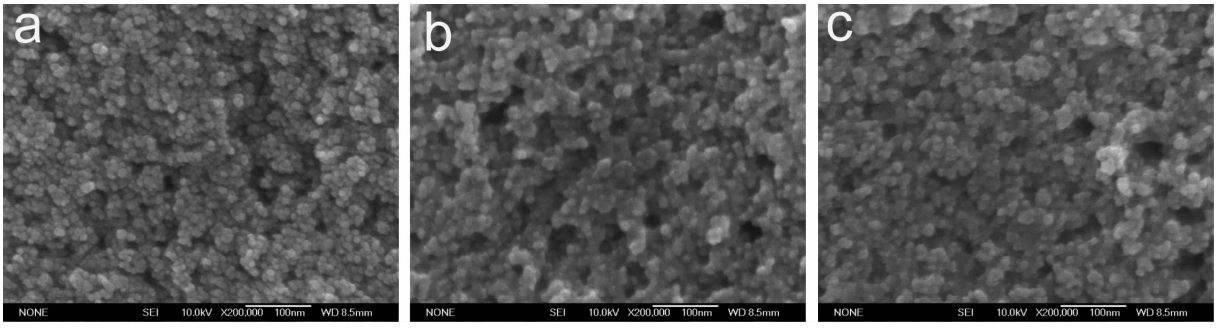

Fig.5 SEM images of bare and protein attached $CoFe_2O_4$ nanocrystals: (a) Bare nanocrystals; (b) BSA attached nanocrystals; (c) Hemoglobin attached nanocrystals

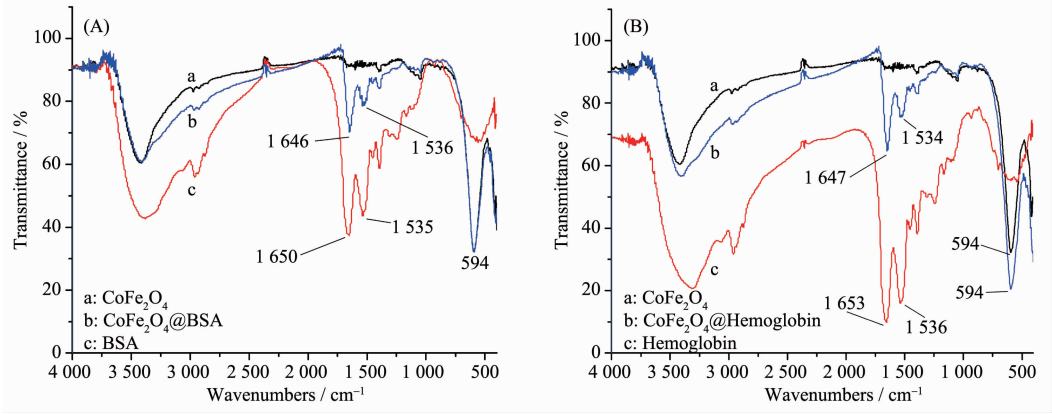

Fig.6　FTIR analysis of protein-nanocrystal interaction in the case of BSA (A) and hemoglobin (B)

2.4　FTIR analysis of protein conformation changes induced by nanocrystal

Vibrations in adjacent chemical groups are often coupled and this coupling correlates to the protein conformation, which makes infrared spectrum a sensitive and effective method for protein structure investigation. Protein molecule has two characteristic vibration bands amide Ⅰ (~1 650 cm^{-1}) and amide Ⅱ (~1 550 cm^{-1}). The amide Ⅰ band originates from C=O stretching vibration and minor out-of-phase CN stretching vibration. Amide Ⅱ also provides protein structure information, but the relation between protein structure and vibration frequency is less straightforward than that of amide Ⅰ band[33].

Fig.6 is the FTIR spectra of protein, nanocrystal and nanocrystal-protein complex. $CoFe_2O_4$ nanocrystals have a characteristic and strong adsorption band at 594 cm^{-1} which is assigned to the vibration between metal and oxygen ion in the crystal lattice[34]. Amide Ⅰ and Ⅱ vibration bands can be obviously seen in the spectra of pure BSA and hemoglobin. After protein being adsorbed to nanocrystals, the spectrum clearly shows the characteristic bands both of protein and cobalt ferrite, which indicates that protein has been successfully attached to the nanocrystals. It can be seen that nanocrystals have caused amide Ⅰ band respectively shifted 4 cm^{-1} and 6 cm^{-1} to lower wavenumbers in the case of BSA and hemoglobin. Whereas amide band Ⅱ only suffers 1 cm^{-1} and 2 cm^{-1} shifting for BSA and hemoglobin. These shifts in IR spectrum imply that protein conformation has been changed by the protein-nanocrystal interaction.

3　Conclusions

Spinel $CoFe_2O_4$ nanocrystals with nanoscale approximately 10 nm were synthesized by hydrothermal method and the mechanism for protein-nanocrystal interaction was investigated using BSA and hemoglobin as model proteins. Nanocrystals efficiently adsorb BSA and hemoglobin with a high capacity of 238 $mg\cdot g^{-1}$ and 257 $mg\cdot g^{-1}$ at an appropriate pH value of 5.5 and 7.0. The relationship between protein adsorption and ζ potential indicates that hemoglobin is adsorbed to nanocrystals via electrostatic interaction whereas BSA adsorption is not agreed with such mechanism. The advantages of high adsorption capacity and diverse adsorption mechanism for different proteins meet the requirements of high efficiency and high selectivity in the field of protein adsorption and separation, which implies that $CoFe_2O_4$ nanocyrstals may be a good candidate of protein adsorbent. BSA and hemoglobin adsorption results in nanocrystal-protein aggregation to different DLS size distributions. This property may be utilized for protein detection based on DLS technique. Nanocrystals also make protein amide Ⅰ band shifted in IR spectrum indicating that protein conformation is changed due to the interactions with nanocrystals. However, the biological consequences should be further studied in order to make sure whether the conformation changes are harmful to protein functions or not. In summary, interactions of protein and $CoFe_2O_4$ nanocrystals lead to protein adsorption to

nanocrystals, nanocrystal-protein complex aggregates and protein conformation changes.

Acknowledgement: We gratefully acknowledge the financial support from the National Natural Science Foundation of China (No.51172085). The authors also acknowledge Electron Microscopy Center of Wuhan University for supporting HRTEM analysis.

References:

[1] Monopoli M P, berg C, Salvati A, et al. *Nat. Nanotechnol.*, **2012**,**7**:779-786

[2] Mahmoudi M, Lynch I, Ejtehadi M R, et al. *Chem. Rev.*, **2011**,**111**:5610-5637

[3] Nel A E, Mdler L, Velegol D, et al. *Nat. Mater.*, **2009**,**8**:543-557

[4] Shemetov A A, Nabiev I, Sukhanova A. *ACS Nano*, **2012**,**6**:4585-4602

[5] Lynch I, Dawson K A. *Nanotoday*, **2008**,**3**:40-47

[6] Walkey C D, Chan W C W. *Chem. Soc. Rev.*, **2012**,**41**:2780-2799

[7] Ge C, Du J, Zhao L, et al. *PNAS*, **2011**,**108**:16968-16973

[8] Hu W, Peng C, Lv M, et al. *ACS Nano*, **2011**,**5**:3693-3700

[9] Gan X, Liu T, Zhong J, et al. *ChemBioChem.*, **2004**,**5**:1686-1691

[10]Zhou H, Gan X, Liu T, et al. *J. Biochem. Biophys. Methods.*, **2005**,**64**:38-45

[11]Zhu X, Yuri I, Gan X, et al. *Biosens. Bioelectron.*, **2007**,**22**:1600-1604

[12]Zhou H, Gan X, Liu T, et al. *Bioelectrochem.*, **2006**,**69**:34-40

[13]Li C, Yang K, Zhang Y, et al. *Acta. Biomater.*, **2011**,**7**:3070-3077

[14]Xu M, Li J, Iwai H, et al. *Sci. Rep.*, **2012**,**2**:1-6

[15]Aubin-Tam M-E, Hamad-Schifferli K. *Biomed. Mater.*, **2008**,**3**:1-17

[16]Mao S, Lu G, Yu K, et al. *Adv. Mater.*, **2010**,**22**:3521-3526

[17]Jia L, Lu Y, Shao J, et al. *Trends. Biotechnol.*, **2013**,**31**:99-107

[18]Rezwan K, Studart A R, Voros J, et al. *J. Phys. Chem. B*, **2005**,**109**:14469-14474

[19]Rabe M, Verdes D, Seeger S. *Adv. Colloid. Interface. Sci.*, **2011**,**162**:87-106

[20]Doane T, Chuang C H, Hill R J, et al. *Acc. Chem. Res.*, **2012**,**45**:317-326

[21]Sanpo N, Berndt C C, Wen C, et al. *Acta. Biomater.*, **2013**,**9**:5830-5837

[22]Kooti M, Saiahi S, Motamedi H. *J. Magn. Magn. Mater.*, **2013**,**333**:138-143

[23]Sharifi I, Shokrollahi H, Amiri S. *J. Magn. Magn. Mater.*, **2012**,**324**:903-915

[24]Franchini M C, Baldi G, Bonacchi D, et al. *Small*, **2010**,**6**:366-370

[25]Kim J I, Chun C J, Kim B, et al. *Biomaterials.*, **2012**,**33**:218-224

[26]Joshi H M, Lin Y P, Aslam M, et al. *J. Phys. Chem. C*, **2009**,**113**:17761-17767

[27]Yoon T J, Kim J S, Kim B G, et al. *Angew. Chem. Int. Ed.*, **2005**,**44**:1068-1071

[28]Scarberry K E, Dickerson E B, McDonald J F, et al. *J. Am. Chem. Soc.*, **2008**,**130**:10258-10262

[29]Bradford M M. *Anal. Biochem.*, **1976**,**72**:248-254

[30]Liu X, Dai Q, Austin L, et al. *J. Am. Chem. Soc.*, **2008**,**130**:2780-2782

[31]Sinkó K, Manek E, Meiszterics A, et al. *J. Nanopart Res.*, **2012**,**14**:894

[32]Chen K, Xu Y, Rana S, et al. *Biomacromolecules*, **2011**,**12**:2552-2561

[33]Barth A. *Biochim. Biophys. Acta*, **2007**,**1767**:1073-1101

[34]Waldron R D. *Phys. Rev.*, **1955**,**99**:1727-1735